213
3/23/70

AEC RESEARCH AND DEVELOPMENT REPORT

1279

Y-1707

Metals, Ceramics, and Materials

MASTER

COMPRESSIVE STRAIN-RATE PROPERTIES OF THORIUM

R. A. Gallman
R. E. Oakes, Jr.

UNION CARBIDE CORPORATION
NUCLEAR DIVISION
OAK RIDGE Y-12 PLANT

operated for the ATOMIC ENERGY COMMISSION under U. S. GOVERNMENT Contract W-7405 eng 26

UNION CARBIDE

OAK RIDGE Y-12 PLANT
P. O. Box Y
OAK RIDGE, TENNESSEE 37830

DISCLAIMER

Printed in the United States of America. Available from Clearinghouse for Federal Scientific and Technical Information, National Bureau of Standards, U.S. Department of Commerce, Springfield, Virginia 22151
Price: Printed Copy $3.00; Microfiche $0.65

Date Issued: March 3, 1970

Document Y-1707

TID-4500

UNION CARBIDE CORPORATION
Nuclear Division

OAK RIDGE Y-12 PLANT

Operated under Contract W-7405-eng-26
With the US Atomic Energy Commission

COMPRESSIVE STRAIN-RATE PROPERTIES OF THORIUM

R. A. Gallman
R. E. Oakes, Jr.

Oak Ridge, Tennessee

Document Y-1707

TID-4500

DISTRIBUTION

Atomic Energy Commission

Keller, C. A.

Lawrence Radiation Laboratory

Westbrook, R. W.

Oak Ridge Gaseous Diffusion Plant

Jordan, R. G.
Wilcox, W. J., Jr.

Oak Ridge Y-12 Plant

Ballenger, H. F. (2)
Beeson, H. C.
Bernander, N. K.
Burkhart, L. E.
Choat, E. E.
Dillon, J. J.
Ebert, J. W.
Ellingson, R. D.
Evans, G. W.
Foulk, D. L.
Gallman, R. A. (5)
Gritzner, V. B.
Haeusler, K. R.
Hemphill, L. F.
Hensley, C. E.
Jackson, V. C.
Kahl, K. G.
Keith, Alvin
Lewis, P. S., Jr.
Mason, D. L.
McLendon, J. D.
Mitchel, G. W.
Myhre, T. C.
Oakes, R. E., Jr. (5)
Oliphant, G. W.
Perry, A. E.
Phillips, L. R.
Smith, R. D.
Stoner, H. H.
Tilson, F. V.
Trotter, T. C.
Warner, J. F.
Waters, J. L.
Wesley, R. L.
Yaggi, W. J.
Y-12 Central Files (5)
Y-12 Central Files (route)
Y-12 Central Files (Y-12RC)

Paducah Gaseous Diffusion Plant

Winkel, R. A.

Sandia-Albuquerque

Ballard, D. W.

Sandia-Livermore

Ingledue, E. F.
Mote, M. W.

In addition, this report is distributed in accordance with the category Metals, Ceramics, and Materials, as given in the "USAEC Standard Distribution Lists for Unclassified Scientific and Technical Reports", TID-4500.

ABSTRACT

The strain-rate dependence of the mechanical properties of thorium in compression at room temperature was studied using an Instron testing machine and a split Hopkinson bar. Results revealed that thorium is strain-rate dependent even at low strain rates.

CONTENTS

SUMMARY

A conventional Instron testing machine and a split Hopkinson bar were employed to investigate the strain-rate dependence of the mechanical properties of thorium in compression at room temperature. The results, which covered a strain-rate range of about seven orders of magnitude, show that thorium is a strain-rate-sensitive material even at low strain rates.

INTRODUCTION

The strain-rate dependence of the mechanical properties of thorium is an important characteristic of parts which are subject to impact loading and those which are fabricated by material-working operations.

In the study of the compressive strain-rate properties of thorium, an Instron testing machine was used over a low strain-rate range; higher compressive strain rates were achieved through a split Hopkinson bar. By combining the test results gathered through the use of these devices, the strain-rate dependence of the mechanical properties of thorium was determined over a strain-rate range of approximately seven orders of magnitude.

COMPRESSIVE STRAIN-RATE PROPERTIES OF THORIUM

STRAIN-RATE MEASUREMENTS

Quasistatic Measurements

For the quasistatic tests, an Instron testing machine was used to compress specimens at low strain rates. The approximate strain-rate range covered by this machine was from 10^{-4} sec^{-1} to 10^{-1} sec^{-1} (crosshead speed from 0.001 to 1.0 in/min).

The experimental arrangement used for measuring large strains is shown in Figure 1. A subpress with a spherical seat was used to obtain axial loading on the specimen. An LVDT-type deflectometer mounted across the compression platens of the subpress was recorded on the X axis of an X-Y recorder, while the load was recorded on the Y axis. From the resulting load-deflection curve, the yield stress and stress at large strains were determined.

Dynamic Measurements

The Hopkinson bar-type tester has been described previously,[1] but some modifications have been made since this report. A schematic diagram of the

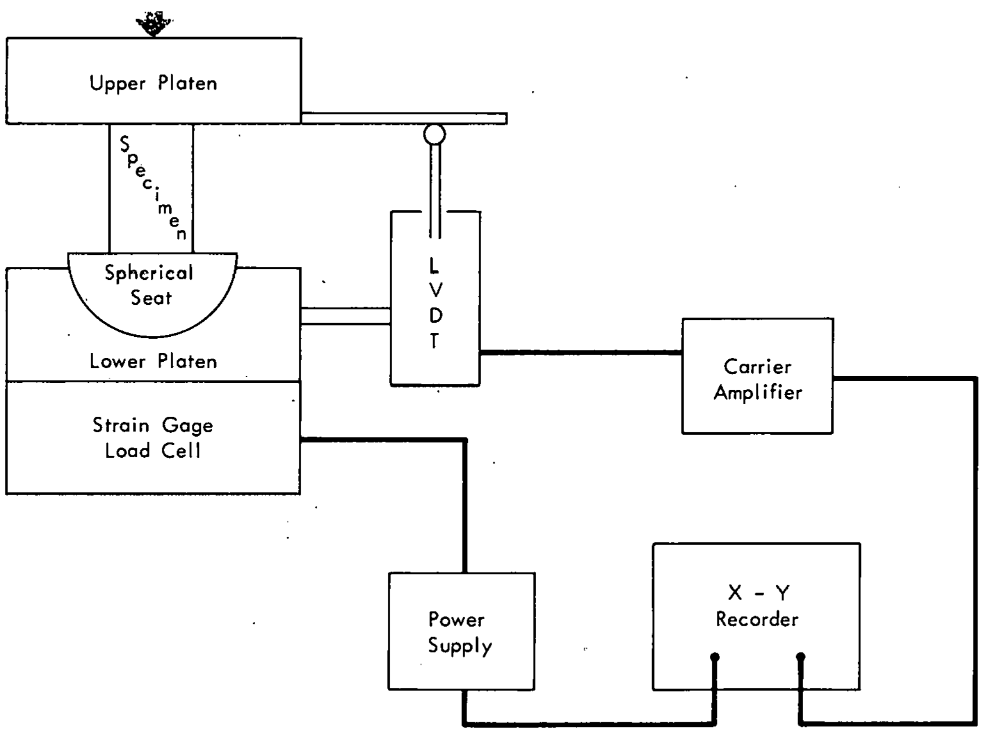

Figure 1. QUASISTATIC EXPERIMENTAL ARRANGEMENT.

apparatus is presented in Figure 2. A gas gun propels a projectile bar into the input pressure bar, sending a longitudinal elastic wave of constant stress level down the bar. The specimen, held in contact and alignment with the input and output bars, will transmit the stress that it is able to support to the output bar. Semiconductor strain gages are mounted on the elastic input and output bars at a distance of 8.5 inches from the bar/specimen interface to record the incident and transmitted stresses, respectively. The data are recorded on a Tektronix 565 dual-beam oscilloscope and preserved on Polaroid film.

The oscilloscope is electrically triggered on impact by completing a circuit between the previously isolated input and output bars and the grounded projectile bar. A delay time is introduced between the impact and the oscilloscope sweep to permit the use of the maximum oscilloscope sweep rate which will record the entire stress pulse duration.

In compression, the output signals from the semiconductor strain gages are nonlinear with respect to stress, so it is necessary to establish an accurate relationship between stress and output voltage. The equation:

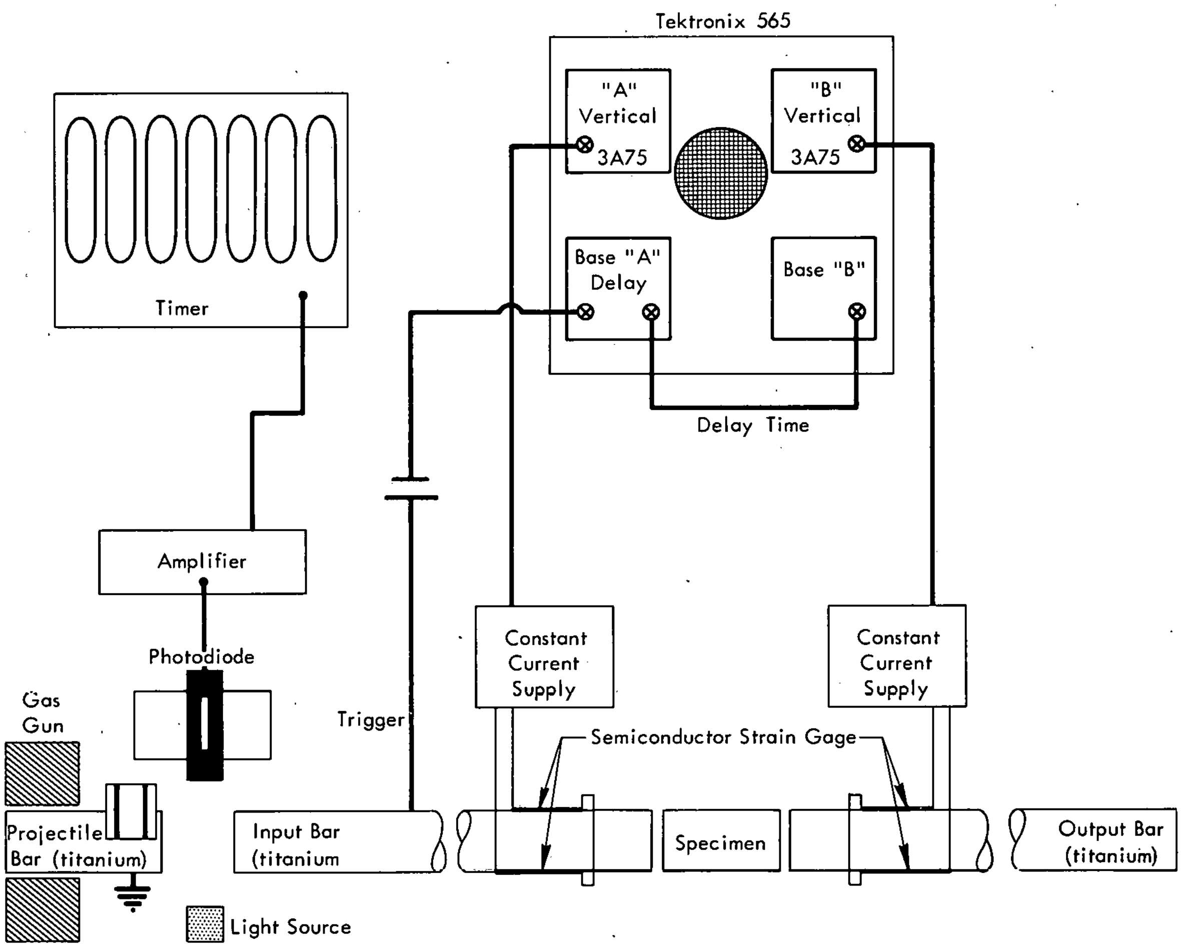

Figure 2. SPLIT HOPKINSON BAR APPARATUS.

$$\sigma = A \ln \left(\frac{B}{B-V}\right),$$

where:

σ represents the stress,

B a constant dependent upon the excitation current and gage resistance,

V the strain gage voltage, and

A a coefficient which must be determined experimentally for each set of gages, has been found to accurately relate voltage output to stress.

To determine the coefficient, A, a series of no-sample tests, with the input and output bars carefully butted together, were conducted at various stress levels, and both strain gages were recorded photographically. The projectile impact velocity was measured by using a light source, a photodiode, and two reference lines mounted on the projectile bar. The reference lines are a known distance apart. As each line crosses between the light source and photodiode, the light path is broken and a pulse transmitted through an amplifier to a timer with the first pulse starting the timer and the second pulse stopping it. Knowing the distance between the reference lines, x, and measuring the time interval required for both lines to pass the photodiode, t, the projectile bar velocity, V, can easlly be found by:

$$V = x/t.$$

From the impact velocity, the stress level introduced into both the input and output bar strain gages can be calculated using the elastic equation:

$$\sigma = \frac{ZV}{2} = \frac{ZX}{2t},$$

where:

Z represents the acoustic impedance of the titanium bars.

The value of the coefficient, A, for each strain gage can then be established by relating input stress with output voltage.

Following this calibration procedure, tests were conducted on a specimen; and the stress, strain rate, and strain determined by the application of the one-dimensional wave propagation theory in elastic bars to the input and output bar stress/time records. If σ_{in} represents the stress which reaches the input bar/specimen interface, part of it is transmitted through the specimen into the output bar, and part is reflected, σ_r. The transmitted stress, σ_t, is recorded by the output bar strain gages. The average stress acting on the specimen at any time is:

$$\sigma_{ave} = 1/2 \left[(\sigma_{in} - \sigma_r) + \sigma_t\right] A_b/A_s,$$

where:

A_b and A_s represent the cross-section areas of the bars and specimen, respectively.

The strain rate, $\dot{\epsilon}$, at any time is the difference between the particle velocities at the bar/specimen interfaces divided by the specimen's length, or:

$$\dot{\epsilon} = \frac{u_{in} - u_{out}}{L},$$

where:

u_{in} and u_{out} represent the particle velocities at the input bar/specimen interface and the output bar/specimen interface, respectively, and

L the length of the specimen.

Since particle velocity and stress are related by:

$$u = \frac{\sigma}{Z},$$

the input bar/specimen interface particle velocity can be expressed as:

$$u_{in} = \frac{(\sigma_{in} - \sigma_r)}{Z},$$

and the output bar/specimen interface particle velocity by:

$$u_{out} = \frac{\sigma_t}{Z}.$$

The strain rate then becomes:

$$\dot{\epsilon} = \frac{(\sigma_{in} - \sigma_r) - \sigma_t}{ZL}.$$

Integration of the strain rate with respect to time then gives the specimen strain, ϵ, or:(2)

$$\epsilon = \int_0^t \dot{\epsilon} dt = \frac{1}{ZL} \int_0^t \left[(\sigma_{in} - \sigma_r) - \sigma_t\right] dt.$$

SPECIMEN MATERIAL AND SPECIFICATIONS

Thorium is the test material investigated in this study. Fabrication involves taking virgin material and forming it into an electrode. The electrode is then double-arc melted, forged, cold rolled, and annealed. The results of a chemical analysis are reported in Table 1. Carbon tends to increase the strength of

Table 1

ANALYTICAL RESULTS ON THORIUM
(All Values in ppm Except Where Noted)

Element	Content
Al	12
B	9
Be	< 3
Bi	< 10
C	310
Ca	35
Cd	< 3
Co	< 1
Cr	12
Cu	20
Mg	< 10
Mn	2
N_2	160
Ni	105
O_2	0.277 wt %
Pb	4
Si	25
Sn	< 4
V	< 1
Zn	< 10
Zr	8

thorium; zirconium which combines with carbon to form carbides tends to decrease the strength. Therefore, as a result of the high carbon content (310 ppm) and the low zirconium content (8 ppm), the net result is an increase in the strength of thorium.

RESULTS

Figure 3 is a plot of the compressive stress versus strain rate for strains between 5 and 20 percent. A plot of the 0.2 percent offset yield stress is also included. The curves are for the convenience of associating the points at a particular strain. A straight horizontal line on this graph would indicate that no strain-rate effect is present, but the plot shows that thorium is strain-rate sensitive even at low strain rates. As is evident, the compressive strength increases with an increase in strain rate. For example, the stress at 5 percent strain increases from 29,400 psi at 0.0000333 sec^{-1} to 55,300 psi at 690 sec^{-1}, an increase of 80 percent, which is substantial. Figure 4 shows the stress-strain relationship for thorium at strain rates ranging from 0.0000333 to 900 sec^{-1}. Strain rate for the dynamic-measurements curve is stated as varying from 400 to 900 sec^{-1} because each point on the curve has a different strain rate, but all are included within this range.

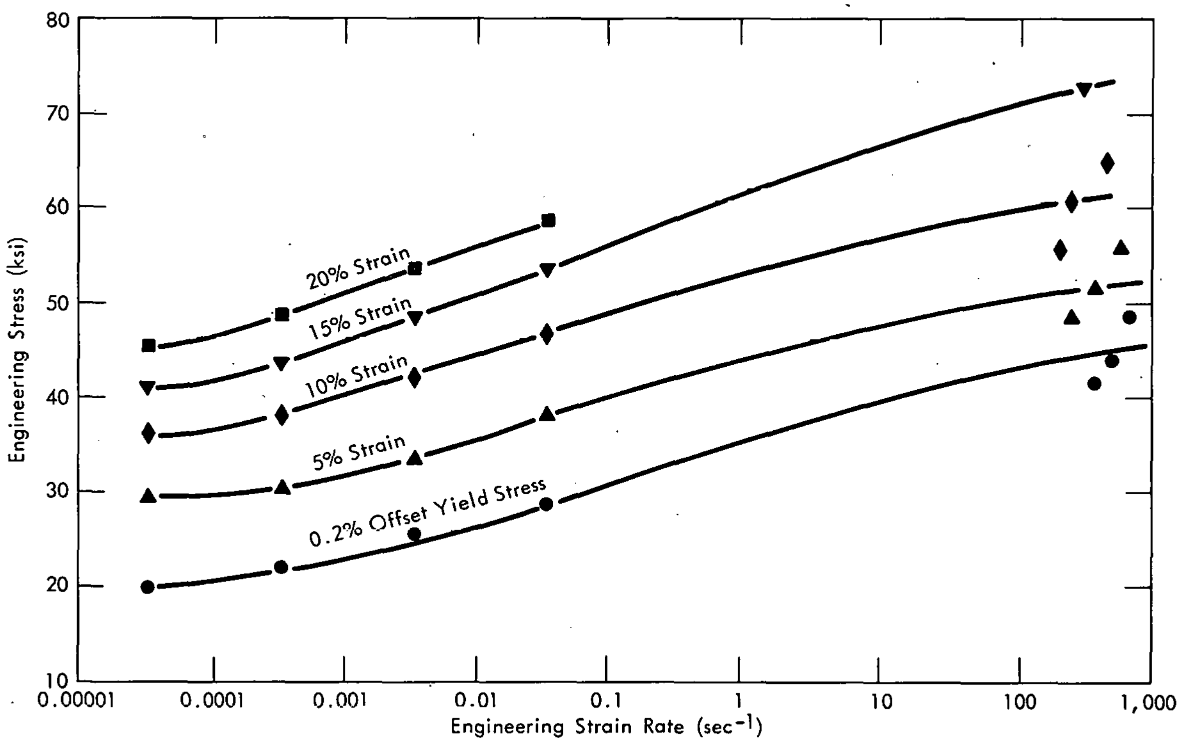

Figure 3. ENGINEERING STRESS AS A FUNCTION OF THE ENGINEERING STRAIN FOR THORIUM COMPRESSION AT ROOM TEMPERATURE.

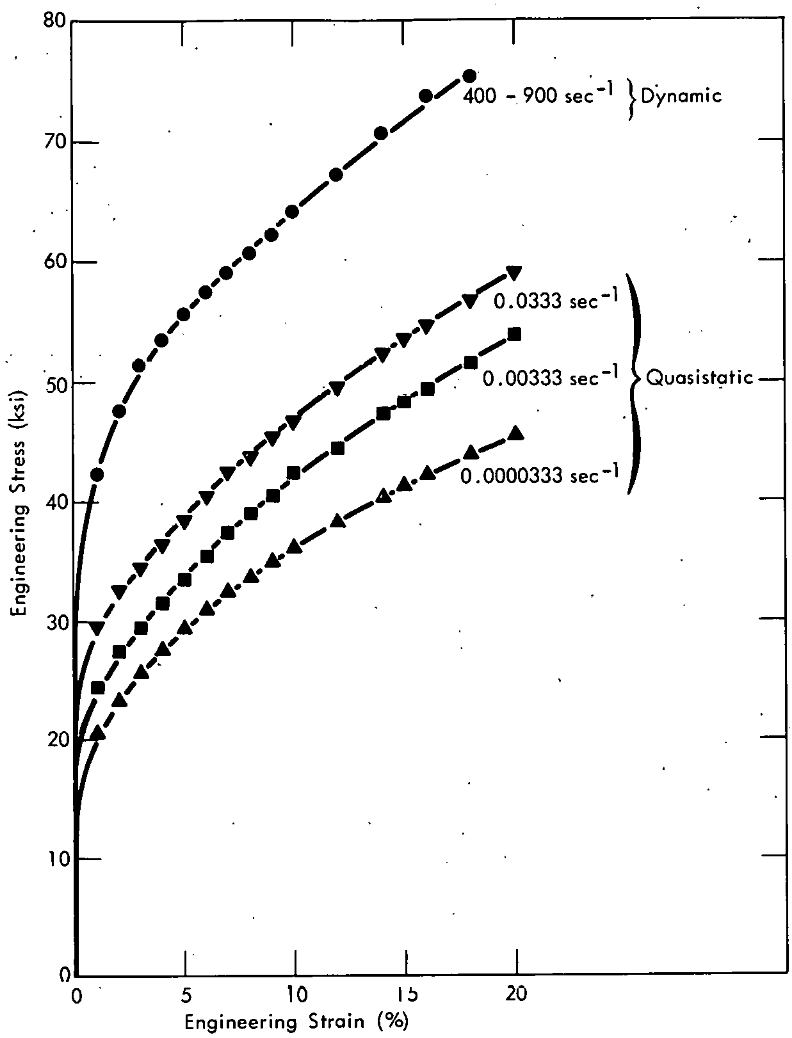

Figure 4. ENGINEERING STRESS AS A FUNCTION OF THE ENGINEERING STRAIN FOR THORIUM IN COMPRESSION AT ROOM TEMPERATURE.

REFERENCES

(1) Hackett, D.W.; Hopkinson Type Strain-Rate Tester, Y-DA-968; Union Carbide Corporation-Nuclear Division, Oak Ridge Y-12 Plant, Oak Ridge, Tennessee; July 23, 1965.

(2) Hauser, F. E. and Winter, C. A.; An Experimental Method for Determining Stress-Strain Relations at High Strain Rates; University of California, MRL Publication, Series 133, Issue 4; December 1960.